Journal of Catalysis 259 (2008) 203–210

Contents lists available at ScienceDirect

Journal of Catalysis

www.elsevier.com/locate/jcat

Combined study of IRMS-TPD measurement and DFT calculation on Brønsted acidity and catalytic cracking activity of cation-exchanged Y zeolites

Takayuki Noda, Katsuki Suzuki, Naonobu Katada, Miki Niwa *

Department of Chemistry and Biotechnology, Graduate School of Engineering, Tottori University, Koyama, Tottori 680-8552, Japan

ARTICLE INFO

Article history:
Received 18 June 2008
Revised 6 August 2008
Accepted 13 August 2008
Available online 6 September 2008

Keywords:
Zeolite
Brønsted acidity
Ammonia
TPD
IR
MS
Ba
Ca
La
Y zeolite
Catalytic cracking
Density functional theory

ABSTRACT

Ammonia infrared spectroscopy/mass spectroscopy-temperature programmed desorption was applied to Ba-, Ca-, and La-exchanged Y zeolites to measure the Brønsted acidity in detail and to gain insight into its relationship to catalytic cracking activity. It was found that the introduced cation located preferentially on sites I′ and/or II replaced the OH in the sodalite cage and hexagonal prism, thereby activating the Brønsted OH in the super cage. The acid strength of Brønsted OH enhanced by the introduced metal cation due to the polarizing effect was confirmed theoretically by density functional calculations. The rate of octane cracking increased with increasing cation exchange, and the turnover frequency on the basis of the number of the active Brønsted OH in the supercage was correlated with the strength of the Brønsted acid site. Thus, the roles of metal cations in Brønsted acidity of Y zeolite was clearly revealed.

1. Introduction

Divalent and trivalent cation-exchanged Y zeolites are well-known catalysts for the cracking of hydrocarbons. In particular, Ca- and La-exchanged Y zeolites have been used for catalytic cracking since the beginning of the petroleum refinery process. Although the Brønsted acid sites in these zeolites seem to play important roles, the generation of such sites and the mechanism of the reaction have not yet been sufficiently explained. Ward explained the generation of Brønsted acidity by a Ca cation in zeolite based on the dissociation of adsorbed water molecule by electrostatic field around Ca^{2+} as follows [1]:

$$Ca(OH_2)^{2+} \rightleftarrows CaOH^+ + H^+.$$

This is in agreement with the generation of acidity by the ion exchange of NaY with Ca cation through hydration at an elevated temperature. The resulting H^+ should be bound to bridging SiOAl, and the bridged OH thus formed is believed to be similar in acid strength to the bridged OH in the proton-type Y (HY) zeolite. Therefore, the Brønsted acid site thus formed is not different from the bridged OH in the proton type Y (HY) zeolite. But in the cracking of hydrocarbons, the HY is inactive or very poor at this activity, whereas the CaY is active. Therefore, the generation of a Brønsted acid site of the CaY could not be fully explained based on the mechanism. In other words, it is not known how the Ca cation-exchanged Y zeolite has strong enough Brønsted acid sites to catalyze the cracking of hydrocarbons.

In a study of Mg and Ca ion-exchanged Y zeolites [2], Ward described how the introduction of the more electropositive smaller cations resulted in a more active catalyst than the introduction of larger cations and showed higher activity of MgY than CaY in the *o*-xylene isomerization. The enhanced activity was attributed primarily to a change in the electrostatic field by divalent cation exchange. Previously, Richardson [3] had proposed an approach to elucidating the high catalytic activity of a cation-exchanged zeolite and noted that the bond strength of Brønsted OH was perturbed by the polarizing effect of the neighboring cations. Although various investigations have been performed [4–7], characterizing the acid sites on these Y zeolites is not easy because of their complex structures, and, consequently, scientific understanding of the catalytic activities has not progressed significantly. Studies on the alkaline cation Y zeolite for catalytic applications [8,9] and quantum chemical calculation [10] have been reported. On the other hand, in a solid-state NMR study, Huang et al. observed the strengthening of

* Corresponding author. Fax: +81 857 31 5256.
E-mail address: mikiniwa@chem.tottori-u.ac.jp (M. Niwa).

0021-9517/$ – see front matter
doi:10.1016/j.jcat.2008.08.004

Brønsted acidity through the introduction of La cation to X and Y zeolites [11].

In the present work, we performed ammonia infrared spectroscopy/mass spectroscopy-temperature programmed desorption (IRMS-TPD) experiments, combined with density functional theory (DFT) calculations, to study the high catalytic activity of alkaline earth divalent (Ca and Ba) and rare earth trivalent (La) cation-exchanged zeolites. IRMS-TPD of ammonia is an advanced, powerful technique for measuring the number and strength of Brønsted acid sites both individually and directly [12–14]. Using this technique, we have already measured the strong Brønsted acidities of many kinds of zeolites, including Ca and La Y zeolites [15]. The strength of the Brønsted OH (heat of ammonia adsorption as the index) can be related to the IR band position, as long as it is located on a large pore of 12- to 8-member rings; the lower the wavenumber, the stronger the Brønsted acidity. The catalytic activity of octane cracking can be related to the strength of acidity, and the turnover frequency (TOF) for octane cracking increases with the strength of the acid site. These findings provide insight into Brønsted acidity and its catalytic activity. On the other hand, we confirmed in a recent study that the heat of adsorption of ammonia on various zeolites, calculated using the DFT method with the embedded 8 T cluster model, agreed well with the experimentally measured one from the IRMS-TPD of ammonia [16]. Furthermore, DFT calculation with periodic boundary conditions has been combined with IRMS-TPD measurement to identify the position and strength of four kinds of Brønsted acid sites in CHA zeolite [17]. We can confirm that combining this experiment with theoretical calculations is a very powerful approach to studying Brønsted acidity in zeolites. In this work, we used both IRMS-TPD measurements and DFT calculations to study the roles of Ba-, Ca-, and La-exchanged cations in enhancing the Brønsted acidity of HY zeolite.

2. Experimental

2.1. Zeolite samples and N_2 adsorption

NaY zeolite with a Si/Al_2 ratio of 5:1 was kindly provided by Catalysts and Chemicals Industries Co. After the NaY zeolite was converted to the NH_4 form using NH_4NO_3, it was treated in a nitrate solution [$Ba(NO_3)_2$, $Ca(NO_3)_2$, or $La(NO_3)_3$] at 353 K for 4 h to prepare an NH_4MY (M = Ba, Ca, or La) zeolite. Changing the concentration of the nitrate in the solution and the number of exchange steps (from 1 to 3) varied the degree of exchange by cation, which was shown by the degree of cation exchange as divalent (Ba and Ca) or trivalent (La) cations in % (e.g., BaHY35). The NH_4MY thus prepared was evacuated at 773 K in an IR cell before the measurement or was treated in N_2 flow for the catalytic cracking. The chemical composition of the exchanged zeolite Y was measured by an inductively coupled plasma spectroscopy after digestion in HF. The nitrogen adsorption isotherm was measured at 77 K using a Bel-sorp mini apparatus.

2.2. IRMS-TPD of ammonia

The IRMS-TPD method has been described in detail previously [12]. The testing apparatus consisted of a glass vacuum line to which an IR spectroscope (Perkin–Elmer Spectrum One) and a mass spectroscope (Pfeiffer Vacuum QME200) were connected. Helium was fed into the IR cell as a carrier gas at 120 ml min^{-1} and pumped from the exit to maintain the line pressure at 25 Torr (1 Torr = 133 Pa).

Before adsorption of ammonia, IR spectra were measured on the evacuated sample at every 10 K from 373 to 773 K during TPD to measure the reference, $N(T)$, with the temperature raised at a ramp rate of 10 K min^{-1}. Adsorption of ammonia was followed by evacuation at 373 K, and IR spectra were repeatedly obtained at every 10 K during TPD to measure the IR absorption due to the adsorbed ammonia, $A(T)$. Difference spectra were calculated as $A(T) - N(T)$, in which IR bands ascribable to ammonia species and hydroxide were observed. Differential change of the IR absorption [i.e., $-\mathrm{d}[A(T) - N(T)]/\mathrm{d}T$] was calculated at the selected wavenumber to be compared with MS-measured TPD (m/e 16). But the OH band position (ν) changed with the temperature (T) linearly in a slope, $\Delta\nu/\Delta T = -0.03$ to -0.05 $cm^{-1}\,K^{-1}$, where $\Delta\nu$ and ΔT represent changes in band position and temperature, respectively. Thus, the band position of OH was corrected using the aforementioned parameter to the wavenumber observed at 373 K.

The method of curve fitting for determining ΔH has been described in detail previously [18]. To use this method, the value of ΔS of entropy change on desorption of ammonia must first be determined. The ΔS determined in a previous study [18] coincided well with ΔS for phase transformation (vaporization) from liquid to gas ammonia, and thus was theoretically supported. But the present IRMS-TPD experiments were not performed under full equilibrium conditions; a very fast flow of helium was fed into the IR cell to avoid the tailing of ammonia due to the structure of the apparatus, and only a small amount of sample was used as an IR wafer. Therefore, ΔS 51 $J\,K^{-1}\,mol^{-1}$, which was corrected experimentally, was used [12].

2.3. Catalytic reaction

The cracking of octane was measured under atmospheric pressure by a continuous-flow method using a Pyrex glass reactor. First, 30 mg of the NH_4-form catalyst was converted into the H-form (*in situ* prepared H-zeolite) in a flow of nitrogen carrier at 773 K for 1 h. Octane at 14 Torr was fed into the reactor in a nitrogen carrier at a flow rate of 40 ml min^{-1} at 773 K, and products were analyzed with a Shimadzu 14A gas chromatograph with a ULBON HP17 capillary column (25 m long, 0.25 mm i.d.). Because the octane conversion was often >10%, an integrated form of the equation was used to measure the reaction rate r, that is,

$$r = \frac{F}{W}\frac{p}{RT}\ln\left(\frac{1}{1 - x/100}\right),$$

where F, W, and R denote the flow rate of gas, the weight of catalyst, and the gas constant (0.0831 L bar $K^{-1}\,mol^{-1}$), respectively. Here p and T were kept constant at 0.019 bar (14 Torr) and 298 K, respectively. The degree of conversion, x (in %), was measured 15 min after the start of the reaction.

2.4. DFT calculation

Calculations were carried out with Dmol^3 software developed by Accelrys Inc. The geometrical parameter for the initial structure of FAU was obtained from the Material Studio 4.0 library. Cluster models of acid centers were cut off from those structures and terminated by H atoms to maintain neutrality; for example, a chemical composition of the calculated CaHY was $CaHAl_3Si_{45}O_{78}H_{36}$. Not only the Brønsted acid site, consisting of 8 T atoms, but also an exchanged cation and neighboring 6-member rings were optimized, whereas surrounding atoms were kept at the original coordinates (details, *vide infra*). The structure of NH_3, H-zeolite (H-Z), and NH_3–H-Z were optimized by generalized gradient approximation (GGA) level using the Becke–Lee–Yang–Parr (BLYP) exchange and correlation functional. Relativistic effects were taken into account by using an all-electron scalar relativistic method. All calculations were performed using the double numerical with polarization (DNP) basis set. The convergence criteria (energy, force, and displacement) were set at 2×10^{-5} Ha, 4×10^{-3} Ha/Å, and 0.005 Å, respectively. The adsorption energy ($E_{ads} > 0$, corresponding to ΔU for

Table 1
Summary for the Brønsted acid sites on cation exchanged Y zeolites and catalytic cracking activity

Sample[a]	Band position of OH (cm^{-1})	Number of Brønsted acid site, A_0 ($mol\,kg^{-1}$)	Strength of Brønsted acid site, ΔH ($kJ\,mol^{-1}$)	Rate of cracking, r ($10^{-3}\,mol\,s^{-1}\,kg^{-1}$)	Turn-over frequency ($10^{-3}\,s^{-1}$)
HY[b]	3648[e]	0.58	108	1.6	1.4
	3625[e]	0.57	110		
	3571	1.1	119		
	3526	0.8	105		
BaHY21	3647	0.6	101		
	3626[e]	0.75	110	3.3	4.4
	3567	0.4	114		
	3539	0.35	110		
BaHY35	3645	0.6	105		
	3632[e]	0.74	118	4.5	6.1
BaHY51	3640[e]	0.82	114	1.2	1.4
BaHY68	3641[e]	0.7	122	0.74	1.1
CaHY14	3646	0.55	107		
	3626[e]	0.51	115	2.7	5.3
	3567	0.35	115		
	3535	0.3	108		
CaHY37[c]	3646	0.55	104		
	3632[e]	0.5	122	6.6	13
CaHY61	3643	0.6	107		
	3633[e]	0.5	120	4.6	9.2
CaHY69	3643	0.35	114		
	3635[e]	0.35	130	3.7	10
CaHY85	3643	0.29	118		
	3635[e]	0.29	133	3.4	12
LaHY22	3647[e]	0.4	117	4.4	4.4
	3626[e]	0.6	118		
	3567	0.4	114		
	3539	0.35	110		
LaHY28[c]	3634[e]	0.93	116	5.3	5.7
	3555	0.55	106		
EDTA-USY[d]	3635	0.39	116		
	3595[e]	0.47	137	13.1	28
	3540	0.27	122		

[a] NH_4 type zeolite was evacuated before use so that the *in situ* prepared H type zeolite was measured.
[b] Ref. [14].
[c] Ref. [15].
[d] Ref. [13].
[e] Regarded as the active site for cracking.

ammonia desorption) was calculated by the following equation: $E_{ads} = (E_{H\text{-}Z} + E_{NH_3}) - E_{NH_4\text{-}Z}$, where $E_{H\text{-}Z}$, E_{NH_3}, and $E_{NH_4\text{-}Z}$ are the total energy of each structure.

3. Results

3.1. Measurements of Brønsted acidity by IRMS-TPD of ammonia

Four kinds of OH were observed on the *in situ* prepared HY zeolite. Because the Y zeolite has only one kind of T site to which four oxygens are bonded in a tetrahedral configuration, four kinds of Brønsted acid sites are structurally possible; one of these has not been confirmed experimentally, however. In our previous study on HY zeolite [14], therefore, four kinds of Brønsted OH, from high to low IR wavenumbers, were assigned to O(1)H, O(1′ or 4)H, O(2)H, and O(3)H, respectively. OH type and cation exchange site nomenclatures, see Supporting information, S4. The location of the O(1′ or 4)H remained uncertain; it could be the site of O(1)H to which one more Al was neighbored or the site of O(4)H, not yet confirmed. O(2)H and O(3)H were located in the sodalite cage and hexagonal prism, respectively. The number and strength of the four kinds of OH in HY were measured individually, as shown in Table 1.

On the BaHY35, the intensity of OH in the sodalite cage and hexagonal prism decreased, and only the OH in the supercage [O(1)H and O(1′ or 4)H] was distinct ca. 3650 cm^{-1}, as shown in Fig. 1. Throughout the present study, a loading of alkaline earth cation preferentially decreased the intensity of OH located in the sodalite cage [O(2)H] and hexagonal prism [O(3)H]. Adsorption of ammonia diminished the intensity of included OH almost completely; the adsorbed NH_4^+ and NH_3 were observed simultaneously.

An enlarged portion of the difference spectra is shown in Fig. 2a. The recovery profiles of the diminished OH show two kinds of OH with different thermal behaviors at 3645 and 3632 cm^{-1}. The change in intensity was analyzed by dividing it into two portions. The differential change of the intensity with respect to temperature was plotted against temperature, as shown in Fig. 3, which we call the IR-TPD of OH. The intensity of OH at 3645 cm^{-1} recovered at lower temperatures, whereas that of OH at 3632 cm^{-1} recovered at higher temperatures. This means that the two kinds of OH have different capabilities to accommodate

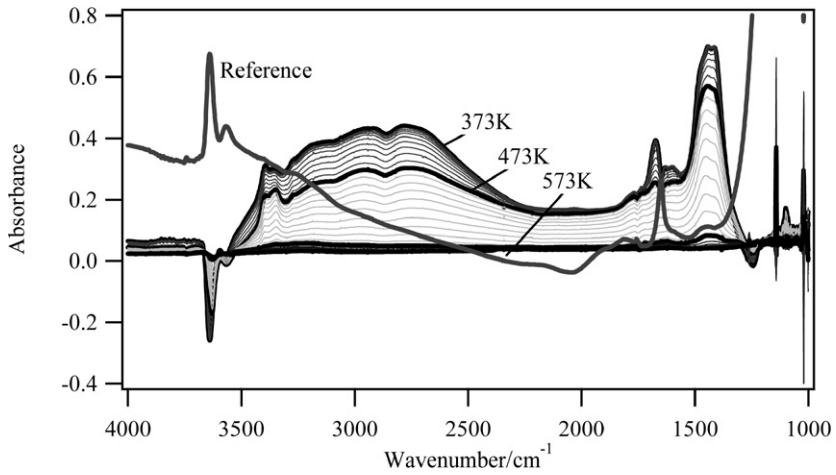

Fig. 1. Difference IR spectra obtained during TPD of ammonia on BaHY35 at 373 to 773 K, altogether with a reference spectrum before adsorption of ammonia measured at 373 K.

an ammonia molecule (i.e., different strengths of acid sites are observed).

As shown in Fig. 2b, an absorption centered at 1440 cm^{-1} was due to the bending vibration of NH_4^+. As mentioned previously [14], this band was assumed to comprise three portions, seen at 1392, 1438, and 1486 cm^{-1}. But the origins of the three NH_4^+ bending vibrations was not known. A differential change in the total intensities is shown in Fig. 3 as an IR-TPD of NH_4^+, corresponding to the thermal change of the Brønsted acid site concentration.

The reference spectrum of the evacuated sample shown in Fig. 1 had an absorption band at ca. 1650 cm^{-1}, the intensity of which depended on such experimental conditions as measurement temperature and concentrations of adsorbed species. This band disturbed measurement of the change of intensity during the TPD experiment and seemed to be due to the Fermi resonance [19]. Because this band was not observed in the spectra after adsorption of ammonia, we calculated the difference spectra $A(T) - A(373)$ (A, absorption; T, temperature), as shown in Fig. 2c, from which the change in intensity of adsorbed NH_3 was calculated at 1661 cm^{-1} to give an IR-TPD of adsorbed NH_3.

Fig. 3 compares of the MS-TPD and IR-TPD thus measured for NH_4^+, NH_3, and OH. Ammonia desorption was observed at low (430 K) and high (520 K) temperature, corresponding to ammonia molecules desorbed from adsorbed NH_3 and NH_4^+, respectively. The sum of the changes in the OH bands was seen to have a compensation relation with that of NH_4^+ to confirm its Brønsted acidity. The number of molecules was measured from desorbed ammonia, and the number of the Brønsted acid sites was quantified. The ΔH of ammonia desorption was measured from the profile of each OH band by a curve fitting method based on the theoretical equation [18]. The parameters measured for the Brønsted acid sites are summarized in Table 1.

In the present study, we studied Ba- and Ca-HY zeolites by changing the degree of exchange. Broadly changing the degree of La cation introduction was difficult, however; therefore, four kinds of BaHY, five kinds of CaHY, and two kinds of LaHY were studied, as shown in Table 1. The data acquisition procedure for CaHY and LaHY was the same as that for BaHY. The solid acidities are summarized in Table 1.

Two OH bands usually were detected in the supercage. The one at the high wavenumber shifted to low and the one at the low wavenumber shifted to high with an increase in the degree of cation exchange. The two OH bands thus merged into an absorption band at ca. 3640 cm^{-1} when more than 50% of Ba cations were introduced. The acid strength, ΔH, was greater for the Brønsted OH band at the lower wavenumber (from 3640 to 3625 cm^{-1}) than that at the higher wavenumber and increased with increasing cation exchange degree, as shown in Fig. 4. ΔH was ca. 5 kJ mol^{-1} greater on CaHY than on BaHY regardless of the exchange degree. For comparison, the data on LaY were plotted altogether.

Fig. 5 summarizes the changes in Brønsted OH associated with the cation exchange degree. The site of OH in the sodalite cage and hexagonal prism on the Ba, Ca, and La cation-exchanged Y zeolites decreased preferentially and diminished at about 40% cation exchange.

3.2. Measurements of activity of octane cracking

Activity of the cracking of octane was measured under monomolecular reaction conditions. We chose a high temperature (773 K) and a low partial pressure of octane (0.019 bar), because the monomolecular reaction was confirmed under these conditions [20]. Catalytic activity was stable for at least for 1 h in all of the samples used. Octane conversion was ca. 10 to 30%; product yields were ca. 35% C_3 and 45% C_4 hydrocarbons, with small amounts of C_5 and C_6 hydrocarbons. Product selectivity did not depend on the sample, but changed slightly with conversion level. Catalyst activities increased and passed through the maximum at ca. 30 to 40% of the Ba- and Ca-exchange levels, as shown in Fig. 6.

Reaction rate was calculated using the equation applicable to an integrated reaction, because the conversion often exceeded 10%. TOF was derived from the rate and the number of the *active* Brønsted acid sites. It was assumed that the Brønsted OH that was located in the supercage and had a greater ΔH was active in the catalytic cracking of octane, as shown in Table 1. Because of similar values of ΔH, two Brønsted OH species in HY and LaHY22 were assumed to be the active sites. The TOF increased with a cation exchange degree of 30 to 40%, but decreased on the BaHY samples with an exchange degree >40% on the Ca samples with an exchange degree of 60%, as shown in Fig. 6.

Fig. 7 illustrates a relationship between TOF of the cracking and ΔH, with the experimental observation on the EDTA-treated USY reported previously [13] was included for comparison. The figure shows that on the cation-exchanged Y zeolites and USY, the TOF of the cracking of octane depended on the strength of the Brønsted acid site located in the supercage. But large deviations from this relationship were found on the BaHY51 and -68, which included large amounts of Ba cation (indicated by the open symbols).

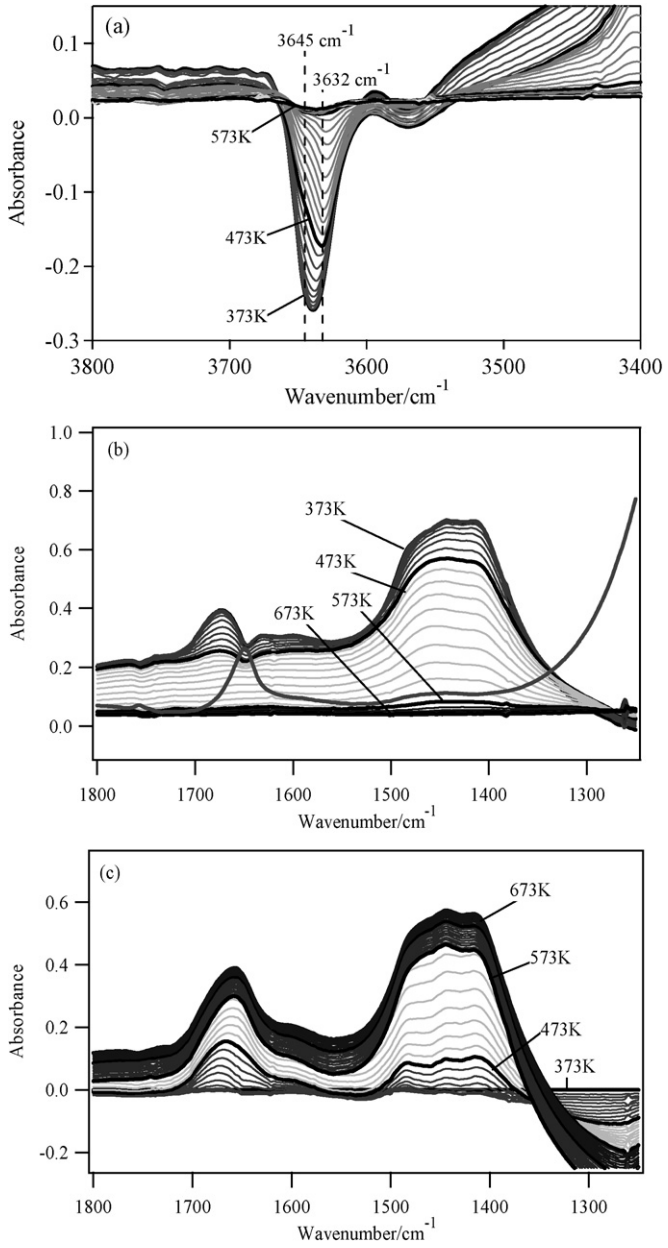

Fig. 2. Enlarged portions of difference spectra in Fig. 1 measured on BaHY35; (a) OH stretching vibration region in 3700–3500 cm^{-1}; (b) ammonia bending vibration region in 1700–1300 cm^{-1}. Difference in $A(T) - A(373)$ in the bending vibration region was shown in (c).

3.3. N_2 adsorption isotherm

Changes in the pore volume due to cation exchange were measured from the adsorption isotherm of nitrogen. All of the isotherms exhibited behavior ascribable to type I, indicating the retained microporosity of the zeolites. But the volume of micropores decreased with the introduction of Ba cation, whereas it remained almost constant in the Ca cation-exchanged Y zeolites, as shown in Fig. 8.

3.4. DFT Calculation of heat of adsorption of ammonia

Sites I and II are known as the principle cation-exchange sites in Ca- and Ba-exchanged Faujasite [21] and X-zeolite [22–24]. These sites are located at a center of double 6 ring (hexagonal prism) and in the supercage adjacent to a single 6 ring, respectively [19].

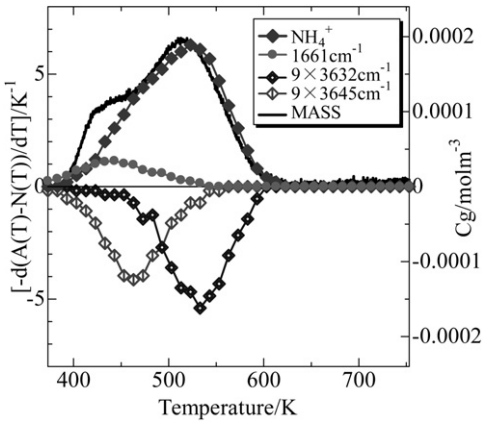

Fig. 3. IR-TPD of OH (3632 and 3645 cm^{-1}), NH_4^+ (1392, 1438, and 1486 cm^{-1}) and NH_3 (1661 cm^{-1}) adsorbed species and its comparison with MS-TPD on BaHY35.

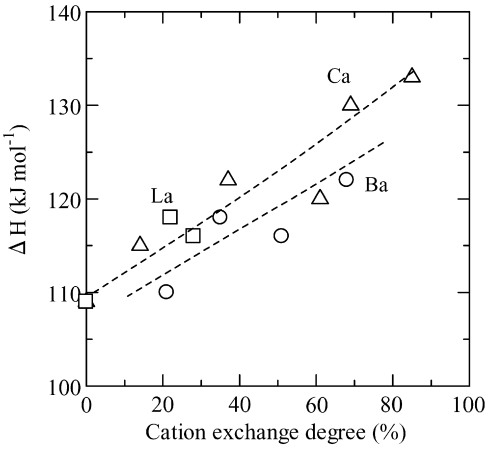

Fig. 4. Change of ΔH of the Brønsted OH located in the super cage at the higher wave number (3625 to 3645 cm^{-1}) with increasing the exchange degree of Ba (○), Ca (△) and La (□) cations.

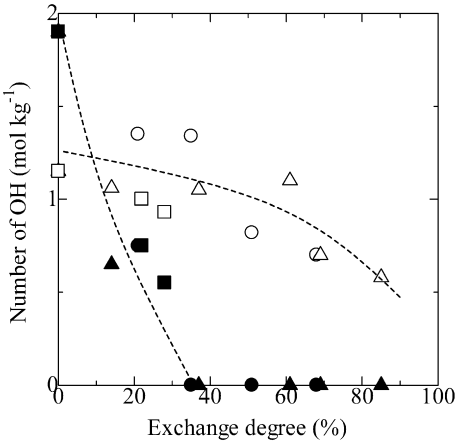

Fig. 5. Change of number of OH in the sodalite cage and double six member ring (closed), and super cage (open) with increasing the exchange degree of Ba (○, ●), Ca (△, ▲) and La (□, ■) cations.

Under hydrated conditions, site I′, located inside the sodalite cage, also has been reported for the cation-exchange site. On the other hand, exchange of the $LaOH^{2+}$ cation at the I′ site also has been postulated [25,26]. The cations, located on sites I and I′ and also on the site II bonds with O(3) and O(2), removed the OH bands below 3570 cm^{-1}. This consideration for metal cation location and OH

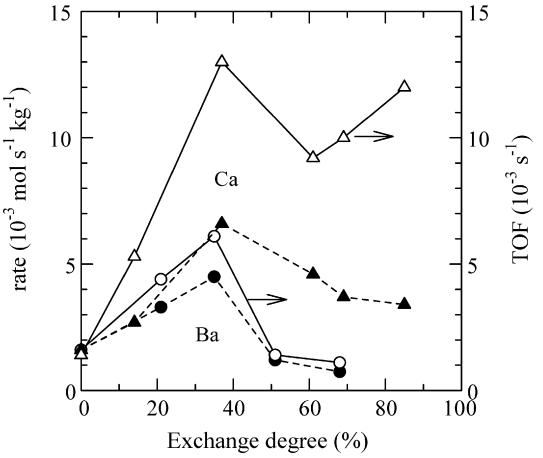

Fig. 6. Change of reaction rate (closed) and TOF (open) with increasing the exchange degree of Ba (○, ●), Ca (△, ▲) cations.

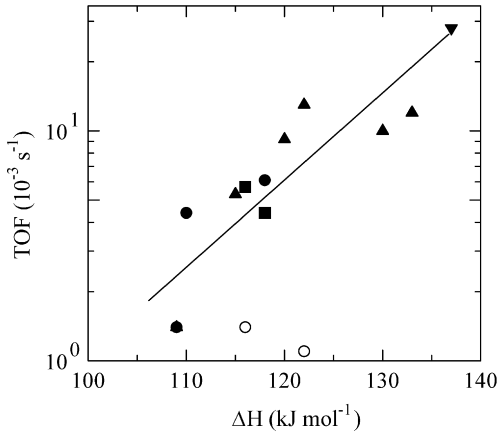

Fig. 7. Relationship between ln(TOF) and ΔH on cation exchanged Y zeolites; BaY (●), CaY (▲), LaY (■) and USY (▼). Open circles show the data on BaHY51 and -68 that included a large amount of Ba cation.

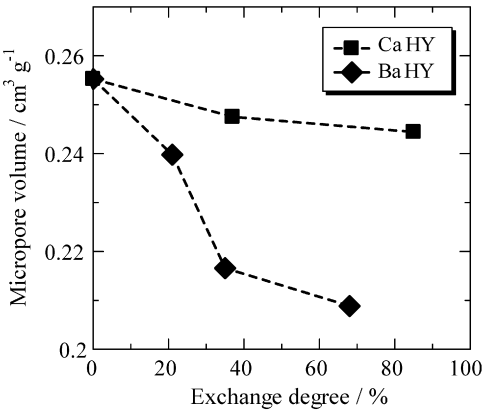

Fig. 8. Change of volume of micropore with increasing the cation exchange degree.

band intensity change coincides with the observations for Brønsted acid sites in the present study, as shown in Fig. 5.

As mentioned earlier, one OH in the supercage observed at ca. 3630 cm^{-1} was activated by cation exchange, but the position of the activated OH site was not fully identified. But because the presence of only O(1)H was confirmed, the O(1)H in the supercage can be assumed to be activated by the introduced cation. Structures of NH_4^+ adsorbed on the metal cation-exchanged Y zeolite were optimized (Fig. 9), and the adsorption energies of NH_4^+ on the O(1) were calculated (Table 2).

Table 2
Calculated heat of adsorption of NH_4^+ on O(1) in the metal cation exchanged Y zeolite and its comparison with the experimentally measured value on BaHY35, CaHY37 and LaHY22

Metal cation	E_{ads} (DFT) (kJ mol^{-1})			ΔH (TPD) (kJ mol^{-1})	ΔU (TPD) (kJ mol^{-1})
	Site I	Site I′	Site II		
(No)	99	100	95	110	106
Ba	116	104	109	118	114
Ca	97	106	116	122	118
LaOH	–	110	–	118	114

ΔH measured by the ammonia IRMS-TPD is equal to $\Delta U + RT$. ΔU, which is slightly smaller than ΔH, is the parameter that should be compared with the calculated energy, E. The Brønsted acid sites calculated here should be compared with those on the exchanged HY zeolites with an ion-exchange degree of ca. 40%, because the OHs in the sodalite cage and hexagonal prism were fully diminished, and the super cage OH was most effectively activated. Comparing the calculated E and ΔU measured on BaHY and CaHY with a ca. 40 % exchange degree showed that the E for sites I′ and II was slightly smaller than ΔU, but the sequences of the energies were the same (i.e., on HY < on BaHY < on CaHY). Therefore, our DFT calculations support the enhanced strength of Brønsted acidity by the exchange of Ba and Ca in sites I′ and II. The adsorption energy of ammonia on the LaHY, in which the LaOH was exchanged on site I′, was 10 kJ mol^{-1} greater than that on the HY. This indicates that our theoretical calculations support the notion that the strength of the Brønsted OH in the supercage was enhanced when Ba and Ca were located in sites I′ and/or II and LaOH was located in site I′. However, the calculated E_{ads} values for the Ca^{2+} located in site I did not exhibited the enhancement expected based on the experimental observations, however.

4. Discussion

4.1. Mechanism of generation of strong Brønsted acidity by the exchanged cation

In this work, we studied the Brønsted acidity of cation-exchanged Y zeolites by IRMS-TPD of ammonia and DFT calculations. Both methods consistently found that the exchanged divalent and trivalent cations enhanced the strength of Brønsted acidity. These metal cations were exchanged with protons in the sodalite cage and hexagonal prism preferentially, and thus the number of Brønsted OHs in these sites decreased gradually. At about a 35% cation exchange degree with Ba and Ca, only two kinds of Brønsted OH were distinctly present in the supercage, and the ΔH of the remaining OH increased gradually. On further exchange with protons in the supercage, ΔH increased. Thus, the enhanced Brønsted acidity can be attributed to the polarizing and inductive effects of the introduced metal cation, as proposed earlier by Richardson [3] and Lunsford [26]. The IRMS-TPD technique has provided the first clear evidence of enhanced Brønsted OH strength due to exchanged cations, and our findings are supported by the DFT calculations.

At a cation exchange degree of >40%, metal cations are exchanged, decreasing the intensity of the OH in the supercage. Under these conditions, sites III and III′ may be exchanged to further increase the ΔH. The detailed mechanism for this remains unclear, however.

The Y zeolite has three different Brønsted OH groups in the hexagonal prism, sodalite, and supercage. OH in the smaller sodalite, supercage, and hexagonal prism acts as an exchangeable site for divalent and trivalent cations. The exchanged cation induces

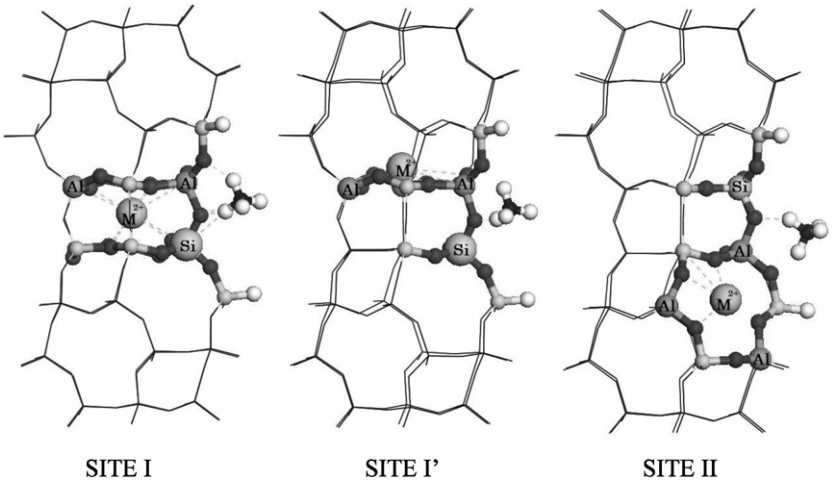

Fig. 9. Structure models of NH_4^+ Brønsted OH activated by M^{2+} cation located on exchange sites, I, I′, and II.

the OH located in the larger supercage to polarize the Brønsted proton. The structure of the exchanged Y zeolite with an M^{2+} exchange degree of ca. 35% is the most typical and is adequate for the active catalytic material with enhanced Brønsted acidity. The Y zeolite pore structure is intrinsically adequate for enhancing the Brønsted acidity based on the present mechanism. The existence of Brønsted/Lewis acid synergy (interaction) remains a matter of active debate in the study of ultrastable Y (USY) zeolite [27–30]. The enhanced activity of USY also may be explained by the inductive effect of extra-framework Al.

Because the ammonium cation is stabilized in bidentate or tridentate in the framework of zeolite [19,31], the measured $-\Delta H$ is not simply equal to the deprotonation energy. The structure of the ammonium cation is an important physicochemical aspect in the study of many kinds of zeolites and may affect the findings. But because the present study deals with the OH in the Y zeolite supercage only on which NH_4^+ is stabilized as the bidentate, our findings are not affected by the structure of NH_4^+.

4.2. Catalytic activity of cation-exchanged Y zeolites

The activity of cracking was found to increase with increasing strength of Brønsted acid sites due to the exchanged cations, Ba, Ca, and La. The cracking activities of BaHY and CaHY went through the maximum, however. The TOF based on the number of Brønsted acid sites showed the maximum at an exchange degree of ca. 30 to 40%. The number of OHs in the supercage decreased when the exchange degree exceeded 40%. This indicates that the decrease in catalytic activity is obviously due to the decrease in the number of the supercage OHs. The decrease in TOF in the region may be caused by the size effect by the cation elements. A nitrogen adsorption isotherm showed a decrease in the micropore volume on the BaHY (Fig. 8). Because Ba^{2+} has a larger cation size than Ca^{2+} (1.98 vs 0.99 Å) [32], Ba^{2+} in the supercage apparently strongly retards the catalytic reaction. Thus, a decrease in the TOF on the introduction of Ba^{2+} into the supercage could be correlated with a less spatial allowance for the catalytic reaction.

The present study on cation-exchanged Y zeolites has an advantage in evaluating the role of Brønsted OH in the cracking of hydrocarbons, because the pore size is kept constant and only the ΔH value changes due to the exchanged alkaline earth cation. Our findings clearly indicate that the enhanced cracking activity on the cation-exchanged zeolites is due to the enhanced acid strength of the Brønsted OH in the supercage.

Another possible explanation for the cracking activity of zeolites has been advanced recently, however [33,34]. This explanation is based on the idea that catalytic activity depends on the adsorption of hydrocarbons more profoundly than on the solid acidity. To reconcile these two concepts for hydrocarbon cracking, a relationship between the hydrocarbon adsorption property and the solid acidity should be studied [35].

5. Conclusion

Based on combined IRMS-TPD of ammonia and theoretical DFT calculations, we have found that <40% of Ba and Ca cations were stabilized in the exchange sites to diminish the OH bands in the sodalite cage and hexagonal prism of the Y zeolite, thereby enhancing the strength of Brønsted OH in the supercage observed at ca. 3620–3635 cm^{-1}. Sites I′ and II are theoretically supported as the cation-exchange sites. The catalytic activity of octane cracking increased with increasing acid strength of the OH. The degree of increase was greater with the exchange by Ca than with that by Ba. The introduction of La stabilized the cation (probably La-OH) on site I′ to enhance Brønsted OH in the supercage and catalytic cracking activity as well. The polarizing effects of the introduced cations may increase the strength of acid sites.

Acknowledgments

This work is supported by a Grant-in-Aid for Scientific Research (A) (18206082) from the Japanese Ministry of Education, Culture, Sports, Science and Technology. We thank Dr. German Sastre, ITQ UPV-CSIC Spain, for fruitful discussions.

Supplementary material

Supporting information for this article may be found on ScienceDirect, in the online version.

Please visit DOI: 10.1016/j.jcat.2008.08.004.

References

[1] J.W. Ward, J. Phys. Chem. 72 (1968) 4211.
[2] J.W. Ward, J. Catal. 17 (1970) 355.
[3] J.T. Richardson, J. Catal. 9 (1967) 182.
[4] C. Mirodatos, P. Pichat, D. Barthomeuf, J. Phys. Chem. 80 (1976) 1335.
[5] A. About-Kais, C. Mirodatos, J. Massardler, D. Barthomeuf, J.C. Vedrine, J. Phys. Chem. 81 (1977) 397.
[6] H.-M. Kao, C.P. Grey, K. Pitchumani, P.H. Lakshminarasimhan, V. Ramamurthy, J. Phys. Chem. 102 (1998) 5627.
[7] K.J. Thomas, V. Ramamurthy, Langmuir 14 (1998) 6687.
[8] J. Xu, B.L. Mojet, J.G. van Ommen, L. Leffert, J. Phys. Chem. B 108 (2004) 15728.
[9] J. Xu, B.L. Mojet, J.G. van Ommen, L. Leffert, J. Catal. 232 (2005) 411.

[10] G.N. Vayssilov, N. Rösch, J. Phys. Chem. B 105 (2001) 4277.
[11] J. Huang, Y. Jiang, V.R.R. Marthala, Y.S. Ooi, J. Weitkamp, M. Hunger, Microporous Mesoporous Mater. 104 (2007) 129.
[12] M. Niwa, K. Suzuki, N. Katada, T. Kanougi, T. Atoguchi, J. Phys. Chem. B 109 (2005) 18749.
[13] M. Niwa, K. Suzuki, K. Isamoto, N. Katada, J. Phys. Chem. B 110 (2006) 264.
[14] K. Suzuki, N. Katada, M. Niwa, J. Phys. Chem. C 111 (2007) 894.
[15] K. Suzuki, T. Noda, N. Katada, M. Niwa, J. Catal. 250 (2007) 151.
[16] K. Suzuki, G. Sastre, N. Katada, M. Niwa, Chem. Lett. 36 (2007) 1034.
[17] K. Suzuki, G. Sastre, N. Katada, M. Niwa, Phys. Chem. Chem. Phys. 9 (2007) 5980.
[18] N. Katada, H. Igi, J.H. Kim, M. Niwa, J. Phys. Chem. B 101 (1997) 5969.
[19] A. Zecchina, L. Marchese, S. Bordiga, C. Paze, E. Gianotti, J. Phys. Chem. B 101 (1997) 10128.
[20] T. Hashiba, D. Hayashi, N. Katada, M. Niwa, Catal. Today 97 (2004) 35.
[21] J.M. Bennett, J.V. Smith, Mater. Res. Bull. 3 (1968) 633.
[22] G. Vitale, L.M. Bull, R.E. Morris, A.K. Cheetham, B.H. Toby, C.G. Coe, J.E. MacDougall, J. Phys. Chem. 99 (1995) 16087.
[23] Y.H. Yeom, S.B. Jang, Y. Kim, S.H. Song, K. Seff, J. Phys. Chem. B 101 (1997) 6914.
[24] Y.H. Yeom, A.N. Kim, Y. Kim, S.H. Song, K. Seff, J. Phys. Chem. B 102 (1998) 6071.
[25] A.K. Cheesam, M.M. Eddy, J.M. Thomas, J. Chem. Soc. Chem. Commun. (1984) 1337.
[26] R. Carvajal, P.-J. Chu, J.H. Lunsford, J. Catal. 125 (1990) 123.
[27] C. Mirodatos, D. Barthomeuf, Chem. Soc. Chem. Commun. (1981) 39.
[28] Q.L. Wang, G. Giannetto, M. Guisnet, J. Catal. 130 (1991) 471.
[29] A. Corma, V. Fornés, F. Rey, Appl. Catal. 59 (1990) 267.
[30] S. Li, A. Zheng, Y. Su, H. Zhang, L. Chen, J. Yang, C. Ye, F. Deng, J. Am. Chem. Soc. 129 (2007) 11161.
[31] E.H. Teunissen, F.B. Vanduijneveldt, R.A. Vansanten, J. Phys. Chem. 96 (1992) 366.
[32] R.T. Sanderson, Inorganic Chemistry, Reinhold Publishing Co., New York, 1967, p. 136.
[33] J.A. van Bokhoven, B.A. Williams, W. Ji, D.C. Koningsberger, H.H. Kung, J.T. Miller, J. Catal. 224 (2004) 50.
[34] B. Xu, C. Sieves, S.B. Hong, R. Prins, J.A. van Bokhoven, J. Catal. 244 (2006) 163.
[35] F. Eder, J.A. Lercher, J. Phys. Chem. B 101 (1997) 1273.